HHS Public Access

Author manuscript

Dev Biol. Author manuscript; available in PMC 2024 August 01.

Published in final edited form as:

Dev Biol. 2023 August ; 500: 10–21. doi:10.1016/j.ydbio.2023.04.007.

Disruption of BMP4 signaling is associated with laryngeal birth defects in a mouse model

N Bottasso-Arias[1], **K Burra**[1], **D Sinner**[1,2,*], **T Riede**[3,*]

[1:] Neonatology and Pulmonary Biology; Perinatal Institute Cincinnati Children's Hospital Medical Center; Cincinnati, Ohio

[2:] College of Medicine, University of Cincinnati, Cincinnati, OH

[3:] Department of Physiology, Midwestern University, Glendale, Arizona

Abstract

Laryngeal birth defects are considered rare, but they can be life-threatening conditions. The *BMP4* gene plays an important role in organ development and tissue remodeling throughout life. Here we examined its role in laryngeal development complementing similar efforts for the lung, pharynx, and cranial base. Our goal was to determine how different imaging techniques contribute to a better understanding of the embryonic anatomy of the normal and diseased larynx in small specimens. Contrast-enhanced micro CT images of embryonic larynx tissue from a mouse model with *Bmp4* deletion informed by histology and whole-mount immunofluorescence were used to reconstruct the laryngeal cartilaginous framework in three dimensions. Laryngeal defects included laryngeal cleft, laryngeal asymmetry, ankylosis and atresia. Results implicate BMP4 in laryngeal development and show that the 3D reconstruction of laryngeal elements provides a powerful approach to visualize laryngeal defects and thereby overcoming shortcomings of 2D histological sectioning and whole mount immunofluorescence.

Graphical Abstract

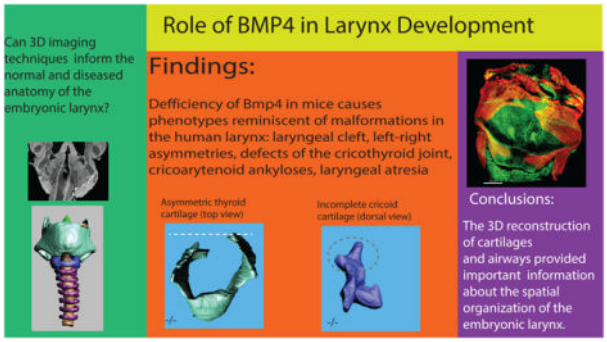

*Correspondence: Debora Sinner; Debora.sinner@cchmc.org , Tobias Riede; triede@midwestern.edu.

Keywords

respiratory airway; cartilage; voice; breathing; swallowing

Introduction

The larynx performs functions for swallowing, breathing and vocal production. A cartilaginous framework and a set of intrinsic muscles provide support to maintain airway patency and facilitate complex movements (Sataloff 2017; Titze 2000). The laryngeal cartilages provide the 'skeleton' of the larynx. Irregularities of their strength, shape, or size can reduce laryngeal lumen or glottal sufficiency causing respiratory stress, complications to swallow, and communication deficits. The shape of each laryngeal cartilage determines the biomechanical properties of the entire framework and its movements (Hunter et al. 2004; Titze, Hunter 2007; Wang 1998). The laryngeal framework must be functional at birth with the first breath (Rutter, Dicksen 2014). Congenital malformations of the larynx belong to a range of craniofacial malformations considered human birth defects (Mossey 2007). According to the Genetic and Rare Diseases Information Center (GARD) at the National Center for Advancing Translational Sciences (NCATS), congenital malformations of the larynx are considered rare (Kaufmann et al. 2018), but they include life-threatening conditions (Landing, Dixon 1979; Daniel 2006; Chang et al. 2021; Lazar et al. 2021; Leonard, Reilly 2021). Mild conditions might not compromise function immediately at birth and are discovered only later in life (Sichel et al. 2000; Merei, Hutson 2002; Bhattacharyya 2015; Shimizu et al. 2018). To inform the etiology of laryngeal birth defects as well as our understanding of normal laryngeal development (Lungova, Thibeault 2020), we conducted this study into the role of a bone morphogenetic protein gene (*BMP4*) in laryngeal development.

Studies in the mouse model demonstrated that laryngeal tissue is of mixed embryological origin (Henick 1993; Tabler et al. 2017; Lungova et al. 2015, 2018; Griffin et al. 2021). Cells of the mesoderm give rise to the cricoid cartilage, arytenoid cartilages, intrinsic laryngeal muscles, and parts of the laminae of the thyroid cartilage (Tabler et al. 2017). Cranial neural crest cells contribute to the formation of connective tissue in the ventral vocal fold lamina propria, most of the thyroid cartilage, and to nervous tissue (Maclean et al. 2008; Tabler et al. 2017; Lungova et al. 2018). The mechanisms by which a range of genes coordinate laryngeal development is little understood (Rutter, Dickson 2014; Lungova et al. 2015).

Bone morphogenetic protein 4 (BMP4) is a protein that is encoded by the *BMP4* gene which is found on chromosome 14q22-q23. In general, bone morphogenetic proteins play roles during embryonic development as well as throughout life. Across species, BMP4 is critical for the development of lung tissue (Weaver et al. 2000), tracheal tissue (Li et al. 2008; Bottasso-Arias et al. 2022), pharyngeal tissue (Bachiller et al. 2003; Szpak 2019), for differentiation of the cranial base (Shum et al, 2003), for limb formation (Duprez et al 1996; Hatakeyama et al, 2004; Pizette, Niswander, 2000) and even for beak shape in songbirds (Abzhanov et al. 2004). Conditional deletion of *Bmp4* in splanchnic mesoderm causes tracheal agenesis (Li et al. 2008) or tracheomalacia with abnormal trachealis muscle

(Bottasso-Arias et al. 2022) and severe defects or asymmetries in the pharyngeal region (Szpak 2019). A role for laryngeal development has not been established before but seems likely given its proximity to and co-occurrence of defects with the aforementioned structures.

Bmp4 expression is enriched in the mesenchyme of the foregut (Li et al, 2008; Domyan et al 2011). The mouse model *Foxg1Cre;Bmp4* was used here, wherein *Bmp4* was conditionally deleted from the foregut and lateral plate mesoderm. We hypothesized that mesodermic components of the larynx would show malformations resulting from ablation of *Bmp4*. To illustrate defects including mild forms of malformations, we employed a recently developed approach that reconstructs the laryngeal cartilaginous framework and the airway in three dimensions. 2D histological sectioning and staining have been the gold standard for assessing tissues but the approach is limited in the evaluation of structural features in 3D. Limitations of 2D imaging approaches include the limited ability to capture asymmetry, the inability of capturing small nuances of shape differences, and limited extent of penetrance of antibodies in whole mount fluorescence (Zukor et al. 2010). To overcome those shortcomings and best capture the three-dimensional complexity of the larynx, we performed contrast-enhanced micro-computed tomographic imaging of the larynx and then reconstructed cartilaginous elements and the laryngeal airway in three dimensions (Riede et al. 2017; Borgard et al. 2020). We also described several cartilaginous and muscle anomalous morphologies associated with the mesenchymal ablation of *Bmp4* in developing mice larynx.

Methods

Mouse breeding and genotyping

Animals were housed in a pathogen-free environment and handled according to the protocols approved by CCHMC Institutional Animal Care and Use Committee (Cincinnati, OH, USA). *Foxg1Cre*;*Bmp4*$^{f/f}$; embryos were generated by breeding *Bmp4* $^{f/f}$ with *Foxg1Cre* mice (Hebert and McConnell 2000) and mating resulting mice to *Bmp4* $^{f/f}$ (B6; 129S4- Bmp4tm1Jfm/J mouse strained was obtained from Jackson Laboratories, stock #016878). This allele of *Bmp4* contains LoxP sites surrounding exon 4, encoding the mature *Bmp4* peptide essential for its function. Mice were maintained in a mix background including 129S4, C57BL/6J, and FVB/NJ Embryos were isolated at E14.5 , E16.5, E18.5, and pups recovered after birth, at P0. Genotypes of transgenic mice were determined by PCR using genomic DNA isolated from embryonic tissue. Primers utilized for genotyping were:

Bmp4 Forward: 5’ GCT AAG TTT TGC TGG TTT GC 3’

Bmp4 Reverse: 5’ GCC CAT GAG CTT TTC TGA GA 3’,

Foxg1Cre Forward: 5’ TGC CAC GAC CAA GTG ACA GCA ATG 3’,

Foxg1Cre Reverse: 5’ AGA GAC GGA AAT CCA TCG CTC G 3’.

microCT imaging, 3D model reconstruction, and geometric morphometric

Whole body scans achieved a resolution of about 10 micrometers per pixel which was insufficient for the segmentation of laryngeal elements. Therefore, larynges were dissected and stained. Tissues were first fixed in formalin solution, then transferred to 99% ethanol (2 days) and then stained in 1% phosphotungstic acid (PTA) (Sigma Aldrich, 79690) in 70% ethanol. After 1 day, the staining solution was renewed, and the tissue was stained for additional 5 days. Specimens were scanned (Skyscan 1172, Bruker) in air positioned inside of a custom-made acrylic tube. The tissue was x-rayed at 3 to 5 micrometer resolution and then segmented using AVIZO software (version Lite 9.0.1) (Figure 1).

The reconstructed image stacks were imported into AVIZO software. Muscle tissue and cartilage have taken up different amounts of PTA and therefore appear brighter or darker in the image (Figure 1D). Laryngeal cartilages were outlined manually (different colors in Figure 1E) and then assembled into a 3D reconstruction for each element. This was repeated for the thyroid cartilage, the cricoid cartilage, both arytenoid cartilages, the epiglottis, and the airway (Figure 1F).

Three linear measures (ventro-dorsal diameter of the cricoid and thyroid cartilage; latero-lateral diameter of the cricoid cartilage), and two cross-sectional areas (airway cross-sectional area at mid-level of the cricoid and the thyroid cartilage) were measured. A one-way between-subjects ANOVA was conducted to compare measures between wildtype, heterozygote, and homozygote fetuses.

Histology, H&E and Alcian Blue Staining

We performed H&E and Alcian blue staining in tissue sections of specimen previously analyzed by microCT imaging. The tissue was destained by keeping it for 8 weeks in neutral buffered formalin. Samples were then processed overnight using a Shandon Excelsior ES tissue processor. Alcohol dehydration and xylene clearing was performed at room temperature. Wax infiltration steps were performed at 62 C. After processing, tissue was embedded in paraffin blocks to generate 7μm sections. For H&E staining, slides were baked for 30 minutes, deparaffinized and rehydrated, and stained with hematoxylin and eosin (Sinner et al 2019). For Alcian blue staining, slides were baked for 30 minutes, deparaffinized, and rehydrated. After a short incubation in 3% Glacial Acetic Acid, slides were stained in Alcian blue for 30 minutes. Nuclear Fast red was utilized for counterstaining. Sections were visualized and photographed using a Nikon wide field microscope coupled with a DS-Fi3 color camera.

Immunofluorescence staining was performed as previously described ((Gerhardt et al. 2018). In brief, antigen retrieval was performed using 10mM Citrate buffer, pH6. Slides were blocked for 2 hours in TBS with 10% Normal Donkey serum and 1% BSA, followed by overnight incubation at 4^0C in the primary antibody, diluted accordingly in blocking solution (See table 1). Slides were washed in 1X TBS-Tween20 and incubated in secondary antibody diluted in blocking solution at room temperature for one hour and were then washed and cover-slipped using Vecta shield mounting media with DAPI. Sections were visualized and photographed using a Nikon wide field microscope coupled with a DS-Fi3 color camera.

Larynx organs were embedded so that coronal sections were performed. However, some malformations were so severe that made it challenging to orient the tissue uniformly and achieve similar looking coronal sections.

Whole mount staining: Larynx-tracheal tissue isolated at E16.5 and E18.5 were subject to whole mount immunofluorescence as previously described (Sinner et al. 2019). Embryonic tissue was fixed in 4% PFA overnight and then stored in 100% MeOH at -20^0C. For staining, wholemounts were permeabilized in Dent's Bleach (4:1:1 MeOH: DMSO: 30%H_2O_2) for 2 hours, then taken from 100% MeOH to 100% PBS through a series of washes. Following washes, whole mounts were blocked in a 2% (w/v) blocking solution (BSA/PBS) for two hours and then incubated, overnight, at 4^0C in primary antibody diluted accordingly in the blocking solution (See Table 1).

After 5 one-hour washes in PBS, whole mounts were incubated with a secondary antibody dilution of 1:500 in blocking solution overnight at 4^0C. Samples were then washed three times in PBS, transferred to 100% methanol and cleared in Murray's Clear (Benzyl benzoate:Benzyl Alcohol 2:1). Images of whole mounts were obtained using confocal microscopy (Nikon A1R). Imaris imaging software was used to convert z-stack image slices obtained using confocal microscopy to 3D renderings of wholemount samples.

Results

3D reconstruction of laryngeal cartilages and airway revealed anomalies in morphology of laryngeal cartilage after mesenchymal deletion of Bmp4.

We have demonstrated the importance of Bmp4 for tracheal cartilage formation and patterning (Bottasso-Arias, et 2022), but it is unknown if Bmp4 influences the development of the laryngeal cartilage. We isolated embryos at E14.5 and E18.5 and subjected them to μCT imaging to analyze the morphology of the cartilaginous elements of the larynx. CTscans from fetuses age E14.5 to E17.5 prenatal day were of insufficient contrast to segment any laryngeal cartilages. The data for E14.5 to E17.5 are not shown. The following qualitative descriptions (summarized in Table 2) are based on observations from four $Bmp4^{f/f}$ (control), four *Foxg1Cre;Bmp4*$^{f/wt}$ (heterozygous) and five *Foxg1Cre;Bmp4*$^{f/f}$ (mutant) fetuses collected from E18.5 and P0.

Thyroid cartilage: Mouse thyroid dorsal horns normally are wide and tend to bend towards the pharyngeal lumen (i.e., towards the mid-sagittal plane) as seen in the control (Figure 2A). In the mutant specimen the dorsal horns were narrow, pointed and did not bend towards the pharyngeal lumen (Figure 2A). The caudal horns were asymmetric in length. In controls the caudal horns point with a ca. 45-degree angle towards the midline and form part of the crico-thyroid joints. In two mutants, the angles were different on the left and the right side causing an asymmetric connection between thyroid and cricoid cartilage.

Cricoid cartilage: The dorsal lamina normally forms a large surface and serves as attachment area for the posterior crico-arytenoid muscle. Clefts or large holes in the dorsal lamina will affect the function of the posterior crico-arytenoid muscle, the only abductor of the vocal folds. In all five mutant mice, the dorsal lamina was incompletely formed (Figure

2B). In one mutant there was a cleft-like gap in the rostral aspect of the dorsal lamina present (Figure 2B). In two specimen we found holes in the dorsal lamina.

The facets for the crico-thyroid joint, sit normally on small protrusions. In mutant mice, the protrusion and the facet were absent or not normally formed, respectively (Figure 2B). The misalignment between the inferior horns of the thyroid cartilage and the facet of the cricoid cartilage, causes a malformation of the crico-thyroid joint (Figure 2B). The cricothyroid joint is a synovial joint between the inferior horn of the thyroid cartilage and the lateral lamina of the cricoid cartilage. Backward and forward rocking movements of the thyroid cartilage causes the vocal folds to stretch or relax. This movement contributes also to vocal fold adduction. The crico-thyroid facets and their protrusion were absent (Figure 2B), and the caudal horns of the thyroid cartilage were not aligned and asymmetric. Both features likely cause a misalignment of the two parts of the joint which will compromise normal movements.

Arytenoid cartilage: The arytenoid cartilage consists of a muscular and vocal process and a long dorsal horn. All three landmarks showed various forms of malformation (Figure 2C). In one mutant, both arytenoid cartilages were fused with the cricoid cartilage (Figure 2C). The crico-arytenoid joint is a true joint and facilitates adduction and abduction of the vocal folds (i.e., opening and closing of the glottis). An ankyloses-like fusion between arytenoid and cricoid cartilage would immobilize the structure.

Trachea: In all five mutants, tracheal rings were missing, and large portions of the trachea were collapsed (Figure 2D).

Laryngeal airway dimensions: In one mutant, the laryngeal lumen was entirely collapsed. Laryngeal airway dimensions in all other specimen were estimated through three distance measures (Cricoid VD, Cricoid LL, and Thyroid VD) and two area measurements (Cricoid area and Thyroid area) (Figure 3). Measurements were on average smaller in the mutant embryo larynx than in heterozygotes and control embryos (Figure 3) (cricoid VD: $F_{(2,13)}=4.37$; $p=0.04$; cricoid LL: $F_{(2,13)}=20.01$; $p<0.001$; cricoid area: $F_{(2,13)}=14.44$; $p<0.001$; thyroid VD: $F_{(2,13)}=8.62$; $p=0.007$; thyroid area: $F_{(2,13)}=20.08$; $p<0.001$).

Taken together, the data support the notion that mesenchymal *Bmp4* is necessary for proper formation of laryngeal cartilage influencing luminal airway dimension.

Histology and whole-mount immunofluorescence demonstrate abnormal organization (orientation) of laryngeal muscles in Bmp4 deficient larynx.

Since CT scan revealed structural cartilaginous anomalies in the larynx, we sought to investigate the extent to which laryngeal cartilage was affected in *Bmp4* deficient larynx. To this purpose we performed alcian blue staining on sections of the samples utilized for CT scanning. Deposition of cartilaginous extracellular matrix was detected in control, heterozygous and homozygote specimen, as determined by alcian blue staining; however, cartilage was much reduced in the mutant specimen (Figure 4). Figure 4 provides sections of examples from all three groups. All samples were embedded to achieve coronal sections but malformations made a consistent embedding difficult. Note that in the homozygote

specimen, the thyroid cartilage is thinner and appears asymmetric confirming the findings of the 3D reconstruction of the same specimen (Figure 4E through H).

Whole-mount immunofluorescence images of younger specimen provide additional information. Major differences were observed in the muscles of the E16.5 mutant larynx. The orientation of the sternohyoideus (ST) muscle is altered in the mutant and partially overlapping with the cricothyroid (CT) muscle that looks enlarged with increasing number of fibers while compared to control *Bmp4*$^{f/f}$ or heterozygous *Foxg1Cre;Bmp4*$^{f/wt}$. Similarly, the right thyrohyoideus (TH) muscle appears to meet at the midline of the thyroid (T) cartilage with its left counterpart TH muscle. Thyroid (T) and cricoid cartilage (C) are hypoplastic. Cricoid cartilage appears collapsed and secondarily affecting the position of the thyroid cartilage (arrowheads in Figure 5A and C) that seems loose as if lacking support. In cross sections of the “distal larynx/proximal trachea the mutant airway appears partially collapse or laterally compressed (Figure 5D) likely reflecting the cartilaginous anomalies detected by whole mount imaging. . Taken together, *Bmp4* deletion affects laryngeal cartilage and muscle organization.

Discussion

We have provided an analysis of laryngeal defects associated with *Bmp4* deletion in a C57BL/6 mouse model. 3D reconstruction of laryngeal cartilages and airway supports a role for Bmp4 in determining the morphology and symmetry of laryngeal cartilages and airway size of larynx and trachea. *Foxg1Cre;Bmp4*-mice presented different phenotypes reminiscent of malformations in the human larynx. Those include laryngeal cleft, left-right asymmetries of thyroid and cricoid cartilages, defects of the cricothyroid joint, cricoarytenoid ankyloses and laryngeal atresia (Atallah et al. 2020; Johnson et al. 2014; Lim et al. 1979; Manning et al. 2005; Montgomery et al. 1955; Rahbar et al. 2006). The defects belong to the most common laryngeal defects in human neonates (Rutter, Dickson 2014; Parkes, Propst 2016) and other species (e.g., Lane 2001; Garrett et al. 2009). In all cases investigated here, the laryngeal defects co-occurred with severe tracheal defects and lung hypoplasia (not shown here but see Bottasso-Arias et al. 2022 for an illustration). However, evaluating the laryngeal defects in isolation without the accompanying tracheal defect, in two embryos would have been fatal (laryngeal atresia) and in another three would likely have caused respiratory complications that in association with the hypoplastic lungs would have not been compatible with life.

In sum, deletion of mesenchymal *Bmp4* in developing mice is responsible directly or indirectly for different laryngeal defects observed in this study.

BMP4 is indispensable for cartilage formation and the symmetry of the laryngeal cartilaginous framework

Laryngeal cleft refers to a condition in which the dorsal aspect of the larynx, i.e., mostly the large lamina of the cricoid cartilage and the space between left and right arytenoid cartilages, is not properly formed and leaves a gap (Figure 6). It is believed that the laryngotracheal cleft is a consequence of an incomplete separation between trachea and esophagus which share a common lumen during early embryological development

(Qi, Beasley 2000; Nasr et al 2019). A tracheoesophageal septum is formed during the early embryological development (Qi, Beasley 2000). If this septum is not formed, the interarytenoid tissue and cricoid cartilage are not formed and a laryngeal cleft follows. The magnitude of the laryngotracheal clefts can vary (Benjamin, Inglis 1989; Cohen 1975; Lim et al. 1979; Holinger et al. 1985). Bmp4 and its antagonistic modulator Noggin, play an important role in the septum formation, i.e., separation between trachea and esophagus (Li et al. 2008; Que at al 2006) and *Bmp4* deletion causes defects like tracheo-oesophageal fistula (Billmyre et al. 2015).

We also observed numerous laryngeal asymmetries in the mouse model. Laryngeal asymmetries summarize a range of observations many of which are associated with a certain degree of glottal insufficiency, i.e., the glottal valve function is compromised (e.g., Belafsky et al. 2002; Eysholdt et al. 2003). Asymmetries can be structural affecting the laryngeal cartilaginous framework (Hirano et al. 1989) or functional affecting neural innervation of laryngeal muscles (Smith et al. 1992). Here we quantified structural asymmetries of the joint between the caudal horns of the thyroid cartilage and the cricoid cartilage. The cricothyroid joint facilitates dorso-ventral as well as cranio-caudal gliding movements (Hunter et al. 2004; Windisch et al. 2010; Hammer et al. 2010) causing an elongation or shortening of the vocal folds. Asymmetry between the left and right joint would limit the movement amplitude and potentially compromise glottal sufficiency (Hunter et al. 2004; Storck, Unteregger 2018).

It seems plausible that the observed asymmetries are a direct consequence of the mesenchymal *Bmp4* deletion. Bmp4 plays a central role in the dorsoventral pattern formation of lung, trachea and pharynx (Dosch et al. 1997; Chen et al. 1997; Onichtchouk et al. 1996). *Bmp4* deletion causes a significant (dorsal to ventral) shift of numerous gene expression patterns (Szpak 2019). Mesenchymal deletion of *Bmp4* in developing lungs causes hypoplasia that is extremely pronounced in the left side, leading to an imbalance in right left pulmonary asymmetry (Bottasso et al. 2022).

Bmp4 plays a crucial role in the dorsoventral orientation of somites including airway structures during the embryological development, (e.g., Kingsley 1994; Sylva et al. 2011; Rankin et al. 2012). A normal distribution of Bmp4 causes the correct dorsoventral concentration of downstream protein coding genes. For example, the expression of *Bmp4* in the ventral tracheal mesenchyme causes (a) the normal chondrogenesis of C-shaped tracheal cartilages that remain open dorsally, (b) a normal smooth muscle layer connecting the dorsal free end points of the C-shaped cartilages and (c) it prevents ectopic muscle tissue spreading into the ventral mesenchyme (Bottasso-Arias et al. 2022). The deletion of *Bmp4* is associated with tracheal agenesis, pulmonary hypoplasia and right left pulmonary asymmetry (Li et al, 2008; Bottasso-Arias et al 2022). Within the developing pharyngeal region there is a high concentration of Bmp4 near the ventral pole (Rankin et al. 2012). Chemically inhibiting Bmp4 in the Xenopus embryo leads to defects in the developing pharynx because the expression of genes which are Bmp4-dependent, shift significantly For example, the genes gcM2, hand1, pax1, and hoxa3 shifted all ventrally in the developing pharyngeal region (Szpak 2019).

A third group of prominent malformations were ankylosis and atresia. We observed two *Bmp4* deficient specimens with cricoarytenoid ankyloses and one with laryngeal atresia. The abnormal fusion of cartilages (ankylosis) or the incomplete chondrogenesis are typical congenital defects associated with *Bmp4* deletion. For example, tracheal rings are abnormally fused or completely absent in the same mouse model (Li et al. 2008; Bottasso-Arias et al. 2022).

Finally, we noted that some laryngeal cartilage was always present, unlike in the trachea organ where cartilage formation is completely absent in most homozygote specimen. The finding may indicate that additional signals provided by the laryngeal epithelium or mesenchyme may also contribute to the specification and differentiation of laryngeal cartilage. For example, epithelial β-catenin activity regulates the differentiation of mesenchymal cell lineages of the trachea, including Sox9 positive cells giving rise to cartilage (Lungova et al 2018; Wendt et al. 2022). We performed a literature review indicating that mutations of several genes are associated with defects in laryngeal chondrogenesis and function in humans (Table 3). Those include members of the Hedgehog (HH) signaling pathway, such as *GLI3* and *SHH*, TGF-beta (*GDF6*) or Retinoic Acid (*ALDH1A2*). Several studies in the mouse have shown the relevance of the HH pathway in development of several organs and particular cartilage of the larynx, trachea, and bronchi (Miller et al. 2004; Snowball et al. 2015a; Nasr et al. 2020). Studies in mice have also demonstrated that ablation of *Macs1*, an enhancer of *Shh*, results in cartilaginous laryngeal malformations (Sagai et al, 2017 Missing citation). Downstream of HH, TGF-bet and WNT signaling, *Sox9* mutations, also associated with campomelic dysplasia, result in laryngotracheomalacia. *Sox9* and its targets *Acan* and *Col2a1*, are critical regulators of chondrogenesis. Their deletion affects the proper formation of cartilage including tracheal and laryngeal cartilage in mice (Akiyama et al. 2002; Bi et al. 1999; Goldring, Tsuchimochi, and Ijiri 2006; Snowball et al. 2015b; Turcatel et al. 2013; Kishimoto et al. 2018). Remarkably, hypermethylation of a genomic region in a network of face- and voice associated genes including *SOX9, ACAN, COL2A1, NFIX* and *XYLT1* may have played a critical role in determining the modern human anatomy of the face and the larynx (Gokhman et al, 2020).

3D reconstruction contributes to phenotyping of the mouse larynx

The absence of a sufficiently described animal model of laryngeal disorders and the challenge to phenotype the vocal organ of small animal models is a well-known problem (Mankarious, Goudy 2010; Thibeault, Welham 2017). Findings of this study illustrate the usefulness of 3D reconstruction of laryngeal elements. The approach allows to capture large malformation but also small nuances of shape differences. It also facilitates the evaluation of functional consequences because a spatial integration of laryngeal elements is possible. The approach opens an avenue into the investigation of laryngeal defects and the role of genetic and environmental factors.

The technique allows phenotyping shape and size of all laryngeal elements during all postnatal stages (Riede et al. 2020; Darwaiz et al. 2022). This study demonstrates the feasibility of CT-image based segmentation in developing embryos. However, the approach

was limited to embryos at E 18.5 and onward. Image resolution was insufficient for segmentation of the larynx in younger stages. Alternative techniques such as micro- and nano-MRI imaging performed in parallel with confocal or multiphoton imaging of whole mount staining might be able to overcome those limits (e.g., Kerckhofs et al. 2014).

Conclusions

The *Bmp4* deletion in a mouse model recapitulated laryngeal defects observed in human neonates. Laryngeal agenesis, laryngeal clefts and stenosis of the laryngeal airway contribute to the neonatal lethality due to respiratory defects. Results suggest a role for BMP4 signaling in laryngeal development, especially in ventro-dorsal patterning and symmetry of the larynx. The 3D reconstruction of laryngeal cartilages and airways provided important complementary information about the spatial organization of structures and thereby overcomes shortcomings of the 2D histological sectioning.

Acknowledgements:

We thank Austin Simister for help with the segmentation. This work has been partially supported by NIH-NHLBI R01 144774, NSF 1754332, and NIH-NIDDK/U24-DK076169-11. The sponsors played no role in study design, in the collection, analysis and interpretation of data, or in the writing of the report.

References

Abzhanov A, Protas M, Grant BR, Grant PR and Tabin CJ, 2004. Bmp4 and morphological variation of beaks in Darwin's finches. Science, 305(5689), 1462–1465. [PubMed: 15353802]

Akiyama H, Chaboissier MC, Martin JF, Schedl A and de Crombrugghe B, 2002. The transcription factor Sox9 has essential roles in successive steps of the chondrocyte differentiation pathway and is required for expression of Sox5 and Sox6. Genes & development, 16(21), 2813–2828. [PubMed: 12414734]

Aramaki M, Udaka T, Kosaki R, Makita Y, Okamoto N, Yoshihashi H, Oki H, Nanao K, Moriyama N, Oku S and Hasegawa T, 2006. Phenotypic spectrum of CHARGE syndrome with CHD7 mutations. The Journal of pediatrics, 148(3), pp.410–414. [PubMed: 16615981]

Atallah I, Manjunath MK, Al Omari A, Righini CA and Castellanos PF, 2019. Cricoarytenoid joint ankylosis: classification and transoral laser microsurgical treatment. Journal of Voice, 33(3), 375–380. [PubMed: 29306525]

Bachiller D, Klingensmith J, Shneyder N, Tran U, Anderson R, Rossant J and De Robertis EM, 2003. The role of chordin/Bmp signals in mammalian pharyngeal development and DiGeorge syndrome. Development 130 (15), 3567–3578. [PubMed: 12810603]

Bargal R, Cormier-Daire V, Ben-Neriah Z, Le Merrer M, Sosna J, Melki J, Zangen DH, Smithson SF, Borochowitz Z, Belostotsky R and Raas-Rothschild A, 2009. Mutations in DDR2 gene cause SMED with short limbs and abnormal calcifications. The American Journal of Human Genetics, 84(1), pp.80–84. [PubMed: 19110212]

Belafsky PC, Postma GN, Reulbach TR, Holland BW and Koufman JA, 2002. Muscle tension dysphonia as a sign of underlying glottal insufficiency. Otolaryngology—Head and Neck Surgery, 127(5), 448–451. [PubMed: 12447240]

Bell SM, Schreiner CM, Wert SE, Mucenski ML, Scott WJ and Whitsett JA, 2008. R-spondin 2 is required for normal laryngeal-tracheal, lung and limb morphogenesis. Development 135 (6), 1049–1058. [PubMed: 18256198]

Benjamin B and Inglis A, 1989. Minor congenital laryngeal clefts: diagnosis and classification. Annals of Otology, Rhinology & Laryngology, 98(6), 417–420. [PubMed: 2729823]

Bhattacharyya N 2015. The prevalence of pediatric voice and swallowing problems in the United States. Laryngoscope 125, 746–750. [PubMed: 25220824]

Bhoj EJ, Haye D, Toutain A, Bonneau D, Nielsen IK, Lund IB, Bogaard P, Leenskjold S, Karaer K, Wild KT and Grand KL, 2019. Phenotypic spectrum associated with SPECC1L pathogenic variants: new families and critical review of the nosology of Teebi, Opitz GBBB, and Baraitser-Winter syndromes. European journal of medical genetics, 62(12), p.103588. [PubMed: 30472488]

Bi W, Deng JM, Zhang Z, Behringer RR and De Crombrugghe B, 1999. Sox9 is required for cartilage formation. Nature genetics, 22(1), 85–89. [PubMed: 10319868]

Bi W, Huang W, Whitworth DJ, Deng JM, Zhang Z, Behringer RR and De Crombrugghe B, 2001. Haploinsufficiency of Sox9 results in defective cartilage primordia and premature skeletal mineralization. Proceedings of the National Academy of Sciences, 98(12), 6698–6703.

Billmyre KK, Hutson M and Klingensmith J, 2015. One shall become two: separation of the esophagus and trachea from the common foregut tube. Developmental Dynamics, 244(3), 277–288. [PubMed: 25329576]

Borgard HL, Baab K, Pasch B and Riede T, 2020. The shape of sound: a geometric morphometrics approach to laryngeal functional morphology. Journal of Mammalian Evolution, 27(3), 577–590.

Bottasso-Arias N, Leesman L, Burra K, Snowball J, Shah R, Mohanakrishnan M, Xu Y, and Sinner D (2022). BMP4 and Wnt signaling interact to promote mouse tracheal mesenchyme morphogenesis. American Journal of Physiology-Lung Cellular and Molecular Physiology 322, L224–L242. [PubMed: 34851738]

Chang DR, Londino AV 3rd and Barnett N, 2021. Multidisciplinary management of a neonate in respiratory distress with undiagnosed type IV laryngeal cleft. Journal of Clinical Anesthesia, 76, 110564–110564. [PubMed: 34695750]

Chen JN, Van Eeden FJ, Warren KS, Chin A, Nusslein-Volhard C, Haffter P and Fishman MC, 1997. Left-right pattern of cardiac BMP4 may drive asymmetry of the heart in zebrafish. Development, 124(21), 4373–4382. [PubMed: 9334285]

Clarke RA, Fang Z, Murrell D, Sheriff T and Eapen V, 2021. GDF6 Knockdown in a Family with Multiple Synostosis Syndrome and Speech Impairment. Genes, 12(9), p.1354. [PubMed: 34573339]

Clifton-Bligh RJ, Wentworth JM, Heinz P, Crisp MS, John R, Lazarus JH, Ludgate M and Chatterjee VK, 1998. Mutation of the gene encoding human TTF-2 associated with thyroid agenesis, cleft palate and choanal atresia. Nature genetics, 19(4), pp.399–401. [PubMed: 9697705]

Cohen SR 1975. Cleft larynx, a report of seven cases. Ann Otol Rhinol Laryngol, 84, 747–56. [PubMed: 1200564]

Daniel SJ, 2006. The upper airway: congenital malformations. Paediatric respiratory reviews, 7, S260–S263. [PubMed: 16798587]

Darwaiz T, Pasch B and Riede T, 2022. Postnatal remodeling of the laryngeal airway removes body size dependency of spectral features for ultrasonic whistling in laboratory mice. Journal of Zoology, 318(2), 114–126.

De Falco F, Cainarca S, Andolfi G, Ferrentino R, Berti C, Criado GR, Rittinger O, Dennis N, Odent S, Rastogi A and Liebelt J, 2003. X-linked Opitz syndrome: Gene and redefinition of the novel mutations in the MID1 clinical spectrum. AMERICAN JOURNAL OF MEDICAL GENETICS PART A, 120(2), pp.222–228.

Domyan ET, Ferretti E, Throckmorton K, Mishina Y, Nicolis SK and Sun X, 2011. Signaling through BMP receptors promotes respiratory identity in the foregut via repression of Sox2. Development, 138(5), pp.971–981. [PubMed: 21303850]

Dosch R, Gawantka V, Delius H, Blumenstock C and Niehrs C, 1997. Bmp-4 acts as a morphogen in dorsoventral mesoderm patterning in Xenopus. Development, 124(12), 2325–2334. [PubMed: 9199359]

Dragatsis I, Ghezzi D, Sevilla T, Cirak S, Wang H, Kaçar Bayram A, Sprute R, Ozdemir O, Cooper E, Pergande M and Efthymiou S, Genotype-Phenotype Correlations in Charcot-Marie-Tooth Disease Due to MTMR2 Mutations and Implications in Membrane Trafficking.

Duprez D, Bell EJDH, Richardson MK, Archer CW, Wolpert L, Brickell PM, and Francis-West PH, 1996. Overexpression of BMP-2 and BMP-4 alters the size and shape of developing skeletal elements in the chick limb. Mechanisms of development, 57(2), 145–157. [PubMed: 8843392]

Eysholdt U, Rosanowski F and Hoppe U, 2003. Vocal fold vibration irregularities caused by different types of laryngeal asymmetry. European Archives of Oto-rhino-laryngology, 260(8), 412–417. [PubMed: 12690514]

Garrett KS, Woodie JB, Embertson RM and Pease AP, 2009. Diagnosis of laryngeal dysplasia in five horses using magnetic resonance imaging and ultrasonography. Equine veterinary journal, 41(8), 766–771. [PubMed: 20095224]

Gerhardt B, Leesman L, Burra K, Snowball J, Rosenzweig R, Guzman N, Ambalavanan M and Sinner D, 2018. Notum attenuates Wnt/β–catenin signaling to promote tracheal cartilage patterning. Developmental biology 436(1), 14–27. [PubMed: 29428562]

Goldring MB, Tsuchimochi K and Ijiri K, 2006. The control of chondrogenesis. Journal of cellular biochemistry, 97(1), 33–44. [PubMed: 16215986]

Gokhman D, Nissim-Rafinia M, Agranat-Tamir L, Housman G, García-Pérez R, Lizano E, Cheronet O, Mallick S, Nieves-Colón MA, Li H and Alpaslan-Roodenberg S, 2020. Differential DNA methylation of vocal and facial anatomy genes in modern humans. Nature communications, 11(1), 1–21.

Gordon CT, Petit F, Kroisel PM, Jakobsen L, Zechi-Ceide RM, Oufadem M, Bole-Feysot C, Pruvost S, Masson C, Tores F and Hieu T, 2013. Mutations in endothelin 1 cause recessive auriculocondylar syndrome and dominant isolated question-mark ears. The American Journal of Human Genetics, 93(6), pp.1118–1125. [PubMed: 24268655]

Griffin K, Pedersen H, Stauss K, Lungova V and Thibeault SL, 2021. Characterization of intrauterine growth, proliferation and biomechanical properties of the murine larynx. PloS one, 16(1), e0245073. [PubMed: 33439907]

Van Haelst MM, Scambler PJ and Hennekam RC, Fraser Syndrome Collaboration Group. Fraser syndrome: a clinical study of, 59, pp.3194–203.

Haddad RA, Clines GA and Wyckoff JA, 2019. A case report of T-box 1 mutation causing phenotypic features of chromosome 22q11. 2 deletion syndrome. Clinical Diabetes and Endocrinology, 5(1), pp.1–4. [PubMed: 30693099]

Hammer GP, Windisch G, Prodinger PM, Anderhuber F and Friedrich G, 2010. The cricothyroid joint—functional aspects about different types of its structure. Journal of Voice, 24(2), 140–145. [PubMed: 19185450]

Hatakeyama Y, Tuan RS and Shum L, 2004. Distinct functions of BMP4 and GDF5 in the regulation of chondrogenesis. Journal of cellular biochemistry, 91(6), 1204–1217. [PubMed: 15048875]

Hebert JM, and McConnell SK. 2000. Targeting of cre to the Foxg1 (BF-1) locus mediates loxP recombination in the telencephalon and other developing head structures. Developmental biology 222 (2): 296–306. [PubMed: 10837119]

Henick DH, 1993. Three-dimensional analysis of murine laryngeal development. Annals of Otology, Rhinology & Laryngology, 102(3_suppl), 3–24.

Hirano M, Yukizane K, Kurita S and Hibi S, 1989. Asymmetry of the laryngeal framework: a morphologic study of cadaver larynges. Annals of Otology, Rhinology & Laryngology, 98(2), 135–140. [PubMed: 2916824]

Holinger LD, Tansek KM and Tucker GF Jr, 1985. Cleft larynx with airway obstruction. Annals of Otology, Rhinology & Laryngology, 94(6), 622–626. [PubMed: 4073742]

Hunter EJ, Titze IR and Alipour F, 2004. A three-dimensional model of vocal fold abduction/adduction. The Journal of the Acoustical Society of America, 115(4), 1747–1759. [PubMed: 15101653]

Johnston DR, Watters K, Ferrari LR and Rahbar R, 2014. Laryngeal cleft: evaluation and management. International journal of pediatric otorhinolaryngology, 78(6), 905–911. [PubMed: 24735606]

Johnston JJ, Sapp JC, Turner JT, Amor D, Aftimos S, Aleck KA, Bocian M, Bodurtha JN, Cox GF, Curry CJ and Day R, 2010. Molecular analysis expands the spectrum of phenotypes associated with GLI3 mutations. Human mutation, 31(10), pp.1142–1154. [PubMed: 20672375]

Kaufmann P, Pariser AR and Austin C, 2018. From scientific discovery to treatments for rare diseases–the view from the National Center for Advancing Translational Sciences–Office of Rare Diseases Research. Orphanet journal of rare diseases, 13(1), 1–8. [PubMed: 29301541]

Kaur P, Chaudhry C, Neelam H and Panigrahi I, 2021. Bardet-Biedl syndrome presenting with laryngeal web and bifid epiglottis. BMJ Case Reports CP, 14(1), p.e236325.

Kelly RG, Jerome-Majewska LA and Papaioannou VE, 2004. The del22q11. 2 candidate gene Tbx1 regulates branchiomeric myogenesis. Human molecular genetics, 13(22), pp.2829–2840. [PubMed: 15385444]

Kerckhofs G, Sainz J, Maréchal M, Wevers M, Van de Putte T, Geris L and Schrooten J, 2014. Contrast-enhanced nanofocus X-ray computed tomography allows virtual threedimensional histopathology and morphometric analysis of osteoarthritis in small animal models. Cartilage, 5(1), 55–65. [PubMed: 26069685]

Kingsley DM, 1994. What do BMPs do in mammals? Clues from the mouse short-ear mutation. Trends in Genetics, 10(1), 16–21. [PubMed: 8146910]

Kishimoto K, Tamura M, Nishita M, Minami Y, Yamaoka A, Abe T, Shigeta M and Morimoto M, 2018. Synchronized mesenchymal cell polarization and differentiation shape the formation of the murine trachea and esophagus. Nature communications, 9(1), 1–13.

Landing BH, Dixon LG 1979. Congenital Malformations and Genetic Disorders of the Respiratory Tract. American Review of Respiratory Disease, 120(1), 151–185 [PubMed: 380420]

Lane JG, 2001, July. Fourth branchial arch defects in Thoroughbred horses: A review of 60 cases. In Proceedings of Second World Equine Airways Symposium (pp. 1–15).

Lau CL, Chee YY, Chung BHY and Wong MSR, 2020. CHARGE syndrome patient with novel CHD7 mutation presenting with severe laryngomalacia and feeding difficulty. BMJ Case Reports CP, 13(7), p.e233037.

Lazar MS, Singh A, Ghai B and Chauhan R, 2021. Malformed cricoid cartilage causing congenital subglottic stenosis: A rare case report. Trends in Anaesthesia and Critical Care, 36, 52–54.

Lee YH and Saint-Jeannet JP, 2011. Sox9 function in craniofacial development and disease. genesis, 49(4), pp.200–208. [PubMed: 21309066]

Leon E, Nde C, Ray RS, Preciado D and Zohn IE, 2023. ALDH1A2-related disorder: A new genetic syndrome due to alteration of the retinoic acid pathway. American Journal of Medical Genetics Part A, 191(1), pp.90–99. [PubMed: 36263470]

Leonard JA and Reilly BK, 2021. Laryngomalacia in the Premature Neonate. NeoReviews, 22(10), e653–e659. [PubMed: 34599063]

Li Y, Gordon J, Manley NR, Litingtung Y and Chiang C, 2008. Bmp4 is required for tracheal formation: a novel mouse model for tracheal agenesis. Developmental biology, 322(1), 145–155. [PubMed: 18692041]

Lim TA, Spanier SS and Kohut RI, 1979. Laryngeal clefts: a histopathologic study and review. Annals of Otology, Rhinology & Laryngology, 88(6), 837–845. [PubMed: 517929]

Lungova V, Verheyden JM, Herriges J, Sun X and Thibeault SL, 2015. Ontogeny of the mouse vocal fold epithelium. Developmental biology, 399(2), 263–282. [PubMed: 25601450]

Lungova V, Verheyden JM, Sun X and Thibeault SL, 2018. β-Catenin signaling is essential for mammalian larynx recanalization and the establishment of vocal fold progenitor cells. Development, 145(4), dev157677.

Lungova V, Thibeault SL 2020. Mechanisms of larynx and vocal fold development and pathogenesis. Cellular and Molecular Life Sciences, 1–15.

Maclean G, Dollé P and Petkovich M, 2009. Genetic disruption of CYP26B1 severely affects development of neural crest derived head structures, but does not compromise hindbrain patterning. Developmental dynamics: an official publication of the American Association of Anatomists, 238(3), 732–745. [PubMed: 19235731]

Mainardi PC, 2006. Cri du Chat syndrome. Orphanet Journal of Rare Diseases, 1, p.33. [PubMed: 16953888]

Mankarious LA and Goudy SL, 2010. Craniofacial and upper airway development. Paediatric Respiratory Reviews, 11(4), 193–198. [PubMed: 21109176]

Manning SC, Inglis AF, Mouzakes J, Carron J, Perkins JA 2005. Laryngeal anatomic differences in pediatric patients with severe laryngomalacia. Arch Otolaryngol Head Neck Surg;131(4), 340–343. [PubMed: 15837904]

Merei JM, Hutson JM, 2002. Embryogenesis of tracheo esophageal anomalies: a review. Ped Surgery Int 18, 319–326.

Miller LAD, Wert SE, Clark JC, Xu Y, Perl AKT and Whitsett JA, 2004. Role of Sonic hedgehog in patterning of tracheal–bronchial cartilage and the peripheral lung. Developmental dynamics: an official publication of the American Association of Anatomists, 231(1), 57–71. [PubMed: 15305287]

Montgomery WW, Perone PM, Schall LA 1955. Arthritis of the cricoarytenoid joint. Ann Otol Rhinol Laryngol., 64, 1025–1033. [PubMed: 13283476]

Mossey P, 2007. Epidemiology underpinning research in the aetiology of orofacial clefts. Orthodontics & craniofacial research, 10(3), 114–120. [PubMed: 17651127]

Nasr T, Holderbaum AM, Chaturvedi P, Agarwal K, Kinney JL, Daniels K, Trisno SL, Ustiyan V, Shannon JM, Wells JM and Sinner D, 2021. Disruption of a hedgehogfoxf1-rspo2 signaling axis leads to tracheomalacia and a loss of sox9+ tracheal chondrocytes. Disease models & mechanisms, 14(2), dmm046573.

Nasr T, Mancini P, Rankin SA, Edwards NA, Agricola ZN, Kenny AP, Kinney JL, Daniels K, Vardanyan J, Han L and Trisno SL, 2019. Endosome-mediated epithelial remodeling downstream of Hedgehog-Gli is required for tracheoesophageal separation. Developmental cell, 51(6), 665–674. [PubMed: 31813796]

Onichtchouk D, Gawantka V, Dosch R, Delius H, Hirschfeld K, Blumenstock C and Niehrs C, 1996. The Xvent-2 homeobox gene is part of the BMP-4 signalling pathway controlling dorsoventral patterning of Xenopus mesoderm. Development, 122(10), 3045–3053. [PubMed: 8898218]

Qi BQ, Beasley SW., 2000. Stages of normal tracheo-bronchial development in rat embryos: resolution of a controversy. Dev Growth Differ 42, 145–53. [PubMed: 10830438]

Que J, Choi M, Ziel JW, Klingensmith J and Hogan BL, 2006. Morphogenesis of the trachea and esophagus: current players and new roles for noggin and Bmps. Differentiation, 74(7), 422–437. [PubMed: 16916379]

Parkes WJ and Propst EJ, 2016. Advances in the diagnosis, management, and treatment of neonates with laryngeal disorders. In Seminars in Fetal and Neonatal Medicine (Vol. 21, No. 4, pp. 270–276). WB Saunders. [PubMed: 27049674]

Pizette S and Niswander L, 2000. BMPs are required at two steps of limb chondrogenesis: formation of prechondrogenic condensations and their differentiation into chondrocytes. Developmental biology, 219(2), 237–249. [PubMed: 10694419]

Poulin MA, Laframboise R and Blouin MJ, 2019. Association of bifid epiglottis and laryngeal web with Bardet-Biedl syndrome: a case report. International Journal of Pediatric Otorhinolaryngology, 122, pp.138–140. [PubMed: 31022684]

Rahbar R, Rouillon I, Roger G, Lin A, Nuss RC, Denoyelle F, McGill TJ, Healy GB and Garabedian EN, 2006. The presentation and management of laryngeal cleft: a 10-year experience. Archives of Otolaryngology–Head & Neck Surgery, 132(12), 1335–1341. [PubMed: 17178945]

Rankin SA, Gallas AL, Neto A, Gómez-Skarmeta JL and Zorn AM, 2012. Suppression of Bmp4 signaling by the zinc-finger repressors Osr1 and Osr2 is required for Wnt/β-catenin-mediated lung specification in Xenopus. Development, 139(16), 3010–3020. [PubMed: 22791896]

Riede T, Borgard HL and Pasch B, 2017. Laryngeal airway reconstruction indicates that rodent ultrasonic vocalizations are produced by an edge-tone mechanism. Royal Society Open Science, 4(11), 170976. [PubMed: 29291091]

Riede T, Coyne M, Tafoya B and Baab KL, 2020. Postnatal development of the mouse larynx: negative allometry, age-dependent shape changes, morphological integration, and a size-dependent spectral feature. Journal of Speech, Language, and Hearing Research, 63(8), 2680–2694.

Rutter MJ and Dickson JM, 2014. Congenital Malformations of the Larynx. In Congenital Malformations of the Head and Neck (121–139). Springer, New York, NY.

Sataloff RT 2017. Clinical Assessment of Voice. Second Edition, Plural Publishing

Sevilla T, Jaijo T, Nauffal D, Collado D, Chumillas MJ, Vilchez JJ, Muelas N, Bataller L, Domenech R, Espinós C and Palau F, 2008. Vocal cord paresis and diaphragmatic dysfunction are severe and frequent symptoms of GDAP1-associated neuropathy. Brain, 131(11), pp.3051–3061. [PubMed: 18812441]

Shimizu K, Uno A, Takemura K, Ashida N, Oya R, Kitamura T, Takenaka Y and Yamamoto Y, 2018. A case of adult congenital laryngeal cleft asymptomatic until hypopharynx cancer treatment. Auris Nasus Larynx, 45(3), 640–643. [PubMed: 28943051]

Sichel JY, Dangoor E, Eliashar R, Halperin D., 2000. Management of congenital laryngeal malformations. Am J Otolaryngol, 21, 22– 30. [PubMed: 10668673]

Shi H, Enriquez A, Rapadas M, Martin EM, Wang R, Moreau J, Lim CK, Szot JO, Ip E, Hughes JN and Sugimoto K, 2017. NAD deficiency, congenital malformations, and niacin supplementation. New England Journal of Medicine, 377(6), pp.544–552. [PubMed: 28792876]

Shum L, Wang X, Kane AA and Nuckolls GH, 2004. BMP4 promotes chondrocyte proliferation and hypertrophy in the endochondral cranial base. International Journal of Developmental Biology, 47(6), 423–431.

Sinner DI, Carey B, Zgherea D, Kaufman KM, Leesman L, Wood RE, Rutter MJ, de Alarcon A, Elluru RG, Harley JB and Whitsett JA, 2019. Complete tracheal ring deformity. a translational genomics approach to pathogenesis. American Journal of Respiratory and Critical Care Medicine, 200(10), 1267–1281. [PubMed: 31215789]

Smith ME, Berke GS, Gerratt BR and Kreiman J, 1992. Laryngeal paralyses: Theoretical considerations and effects on laryngeal vibration. Journal of Speech, Language, and Hearing Research, 35(3), 545–554.

Snowball J, Ambalavanan M, Whitsett J, and Sinner D. 2015a. Endodermal Wnt signaling is required for tracheal cartilage formation. Developmental biology 405 (1): 56–70. [PubMed: 26093309]

Snowball J, Ambalavanan M, Cornett B, Lang R, Whitsett J and Sinner D, 2015b. Mesenchymal Wnt signaling promotes formation of sternum and thoracic body wall. Developmental biology, 401(2), pp.264–275. [PubMed: 25727890]

Storck C and Unteregger F, 2018. Cricothyroid joint type as predictor for vocal fold elongation in professional singers. The Laryngoscope, 128(5), 1176–1181. [PubMed: 29114888]

Sylva M, Li VS, Buffing AA, van Es JH, van den Born M, van der Velden S, Gunst Q, Koolstra JH, Moorman AF, Clevers H and van den Hoff MJ, 2011. The BMP antagonist follistatin-like 1 is required for skeletal and lung organogenesis. PloS one, 6(8), e22616. [PubMed: 21826198]

Szot JO, Slavotinek A, Chong K, Brandau O, Nezarati M, Cueto-González AM, Patel MS, Devine WP, Rego S, Acyinena AP and Shannon P, 2021. New cases that expand the genotypic and phenotypic spectrum of Congenital NAD Deficiency Disorder. Human mutation, 42(7), pp.862–876. [PubMed: 33942433]

Szpak A, 2019. A role for Shh and Bmp4 in regulating the dorsal-ventral patterning of the developing pharyngeal region. Thesis, University of Western Ontario.

Tabler JM, Rigney MM, Berman GJ, Gopalakrishnan S, Heude E, Al-Lami HA, Yannakoudakis BZ, Fitch RD, Carter C, Vokes S and Liu KJ, 2017. Cilia-mediated Hedgehog signaling controls form and function in the mammalian larynx. Elife, 6, e19153. [PubMed: 28177282]

Thibeault SL, Welham NV 2017. Strategies for advancing laryngeal tissue engineering. The Laryngoscope 127, 2319–2320. [PubMed: 28581251]

Titze IR and Hunter EJ, 2007. A two-dimensional biomechanical model of vocal fold posturing. The Journal of the Acoustical Society of America, 121(4), 2254–2260. [PubMed: 17471739]

Titze IR., 2000. Principles of voice production. Iowa City, Ia; National Center for Voice and Speech.

Turcatel G, Rubin N, Menke DB, Martin G, Shi W and Warburton D, 2013. Lung mesenchymal expression of Sox9plays a critical role in tracheal development. BMC biology, 11(1), 1–15. [PubMed: 23294804]

Wang RC, 1998. Three-dimensional analysis of cricoarytenoid joint motion. The Laryngoscope, 108(S86), 1–17.

Weaver M, Dunn NR and Hogan BL, 2000. Bmp4 and Fgf10 play opposing roles during lung bud morphogenesis. Development, 127(12), 2695–2704. [PubMed: 10821767]

Wendt KD, Brown J, Lungova V, Mohad V, Kendziorski C and Thibeault SL, 2022. Transcriptome dynamics in developing larynx, trachea, and esophagus. Frontiers in cell and developmental biology, 1319.

Windisch G, Hammer GP, Prodinger PM, Friedrich G and Anderhuber F, 2010. The functional anatomy of the cricothyroid joint. Surgical and radiologic anatomy, 32(2), 135–139. [PubMed: 19809779]

Zhang Q, Zhang LJ, Yuan SS, Quan XJ, Zhang BY and Zhao D, 2021. Hypoparathyroidism Associated with the DNA Variants in Non-Coding Sequence Region of Calcium-Sensing Receptor. Endocrine and Metabolic Science, 5, p.100106.

Zukor KA, Kent DT and Odelberg SJ, 2010. Fluorescent whole-mount method for visualizing three-dimensional relationships in intact and regenerating adult newt spinal cords. Developmental dynamics, 239(11), 3048–3057. [PubMed: 20931649]

Highlights:

- *Bmp4* is necessary for laryngeal cartilage and muscle development.
- Mesenchymal *Bmp4* deletion causes laryngeal defects reminiscent of human pathologies.
- 3D reconstruction of laryngeal elements is feasible in mice embryos.

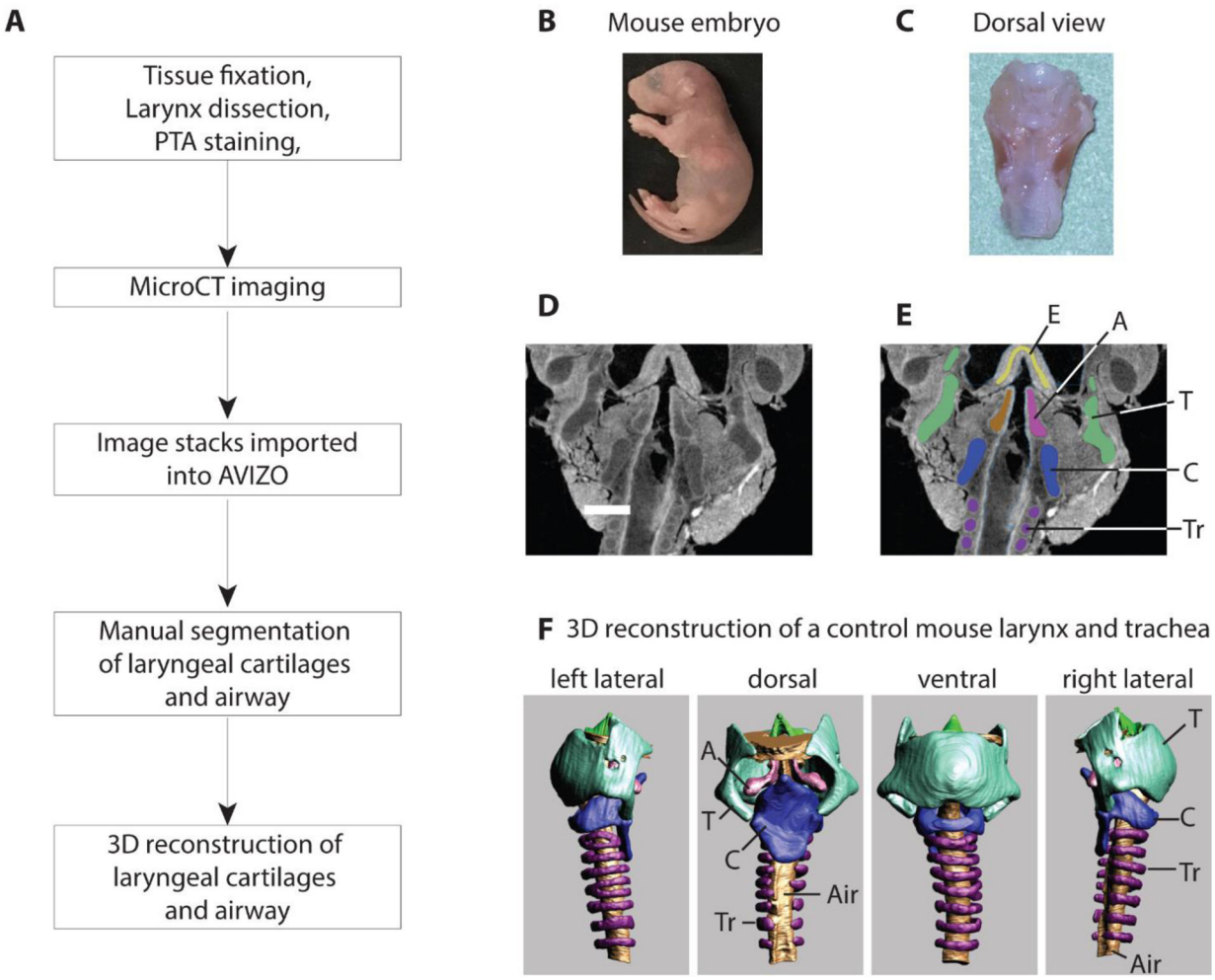

Figure 1:

Workflow for the generation of 3D surface renditions of the mouse larynx (**A**). Mouse fetuses were retrieved at embryological stage E18.5 or P0 (**B**). The larynx was dissected and fixed in neutral buffered formalin, transferred to ethanol, and then stained in a phosphotungstic acid (PTA) solution (**C**). Panels D and E show CT scan images before and after manual segmentation. MicroCT scans were generated at 4 micometer image resolution (**D**). Cartilages and airways were manually outlined (blue-cricoid cartilage; green-thyroid cartilage; lila-tracheal rings; pink and brown – left and right arytenoid cartilage) (**E**). Panel F shows different views of the 3D-surface rendition of larynx and trachea of one control mouse. All laryngeal cartilages and the laryngeal airway were assembled for qualitative and quantitative evaluation (**F**).

T=thyroid cartilage, C=cricoid cartilage, Tr=tracheal ring, Air=airway, A=arytenoid cartilage, E=epiglottis

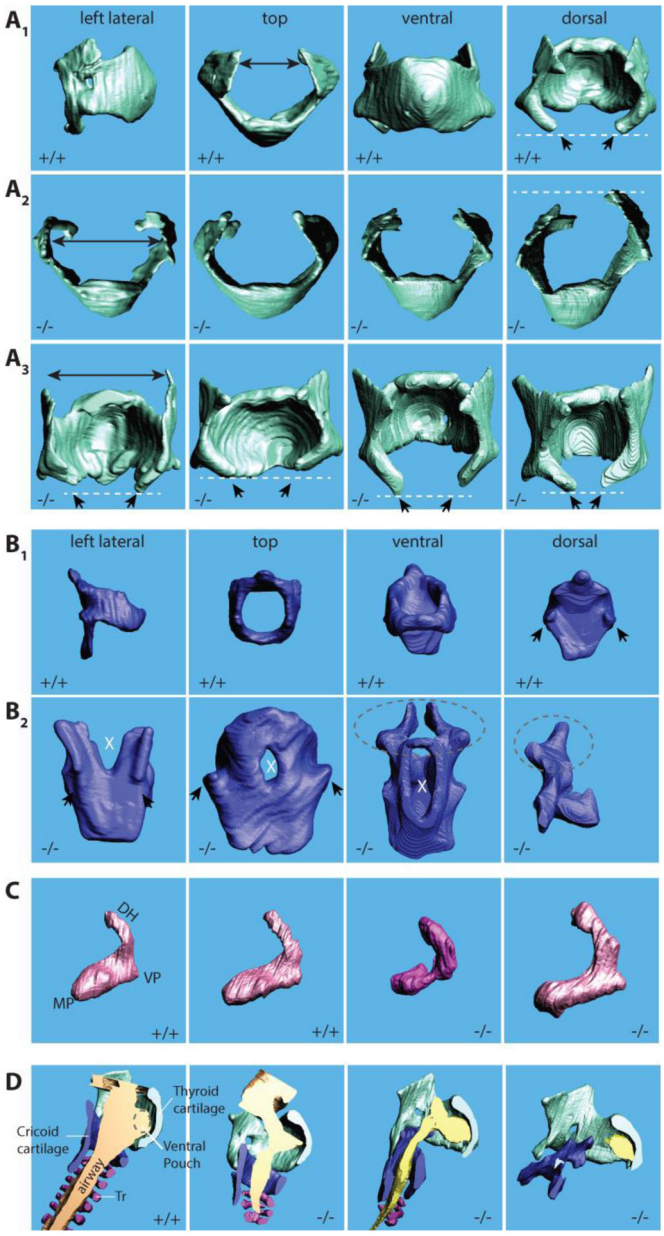

Figure 2:

3D surface renditions of laryngeal cartilages in *Bmp4* $^{f/f}$ (+/+) and *Foxg1Cre; Bmp4* $^{f/f}$ (−/−) fetuses. **A$_{1–3}$**: Thyroid cartilage. **A$_1$**: four views of a thyroid cartilage from a wildtype mouse. 31 Top views (**A$_2$**) and dorsal views (**A$_3$**) of the thyroid cartilage from four homozygote mouse embryos (E 18.5). Note that the dorsal horns are unregular, sometimes pointed and they stand cranially (black arrows). The caudal horns (white dashed lines) are asymmetric and different in length. **B$_{1–2}$**: Cricoid cartilage. **B$_1$**: four views of a cricoid cartilage from a wildtype mouse. **B$_2$**: dorsal views of the cricoid cartilage from four homozygote mouse embryos (E 18.5). Note that in the mutant mice, the dorsal lamina shows a large gap (cleft) or holes (white X). The facets for the articulation with the caudal horns of the thyroid cartilage (black arrows) are absent or malformed. In two embryos the

arytenoid cartilage was fused with the cricoid cartilage (dashed line ellipse). In one embryo, the cricoid cartilage was incomplete (far right image in **B_2**). **C**: Arytenoid cartilage (lateral view of the right cartilage). Deformities of the dorsal horn (DH), muscular (MP) and vocal process (VP). Differences between the left and right cartilage were also noted. **D**: Airways. Laryngeal airways are either reduced or completely collapsed.

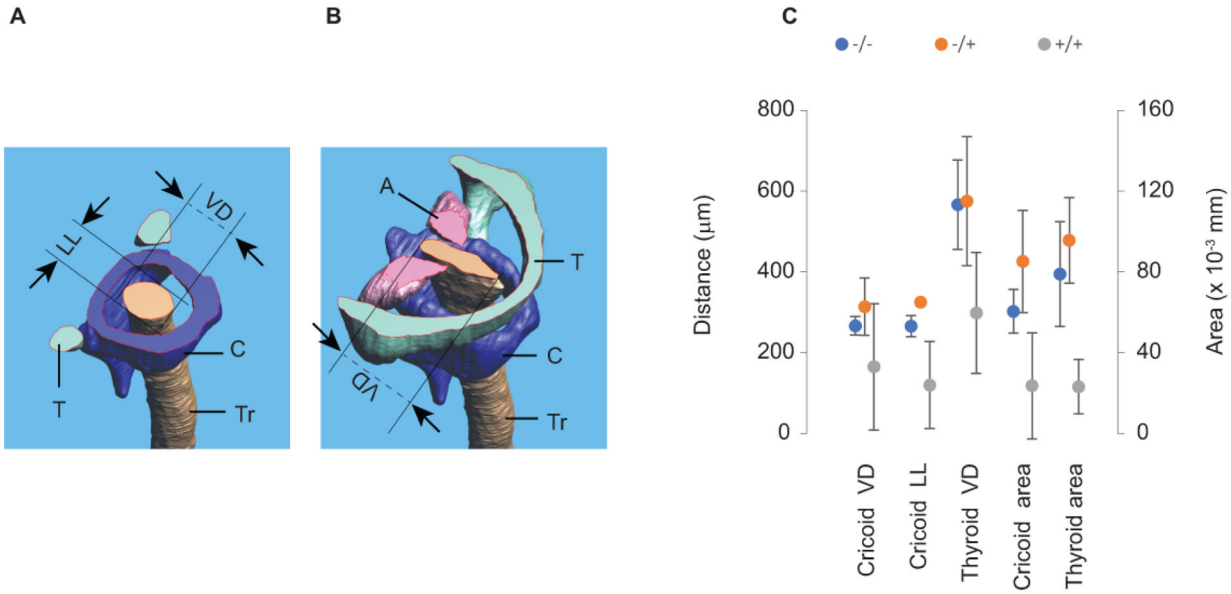

Figure 3:

Laryngeal airway dimensions. Transverse section through the 3D reconstruction of the larynx demonstrating linear dimensions and the area of the airway at the level of the cricoid cartilage (**A**) and the glottal level (**B**). Three distances (Cricoid VD, Cricoid LL, and Thyroid VD) and two airway area measurements (Cricoid area and Thyroid area) were on average, smaller in the mutant mice blue dots (N=5) than in control gray dots (N=4) and heterozygote, orange dots (N=4) pups (**C**).

T= thyroid cartilage; C= cricoid cartilage; Tr= tracheal airway; A= arytenoid cartilage; VD= ventro-dorsal distance of the airway; LL= latero-lateral distance of the airway.

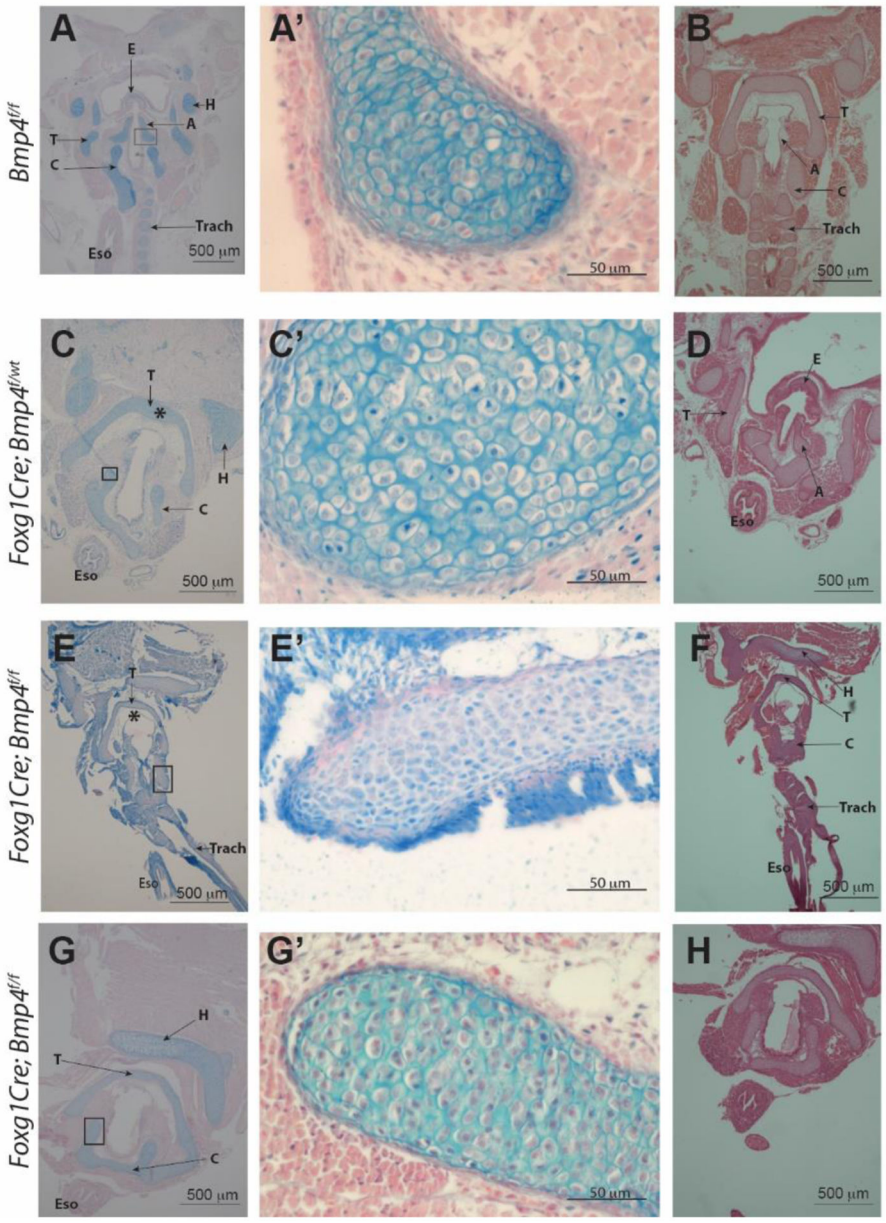

Figure 4:

Histological images of specimen previously used for contrast-enhanced microCT imaging and 3D reconstruction. **A**, **A'**, **B**: Control (*Bmp4* $^{f/f}$) **C**, **C'**, **D**: heterozygote specimen (*Foxg1Cre;Bmp4* $^{f/wt}$). **E-H**: mutant specimen (*Foxg1Cre;Bmp4* $^{f/f}$). Alcian blue staining in left and middle column. H&E stains in **B**, **D**, **F**, and **H**. Abnormal morphology of the larynx resulting from mesenchymal deletion of *Bmp4* is detected in mutant samples. Laryngeal cartilage is present in the mutants (**E** – **H**) but morphology (shape) and thickness of the cartilage elements is not normal (compare thyroid cartilage (*) in panel C vs E). Tracheal cartilage is defective and mostly absent in mutants (compare panel E vs A). T= thyroid cartilage C= cricoid cartilage, A= arytenoid cartilage, E= epiglottis, H= basihyoid bone, Eso= esophagus, Trach= trachea.

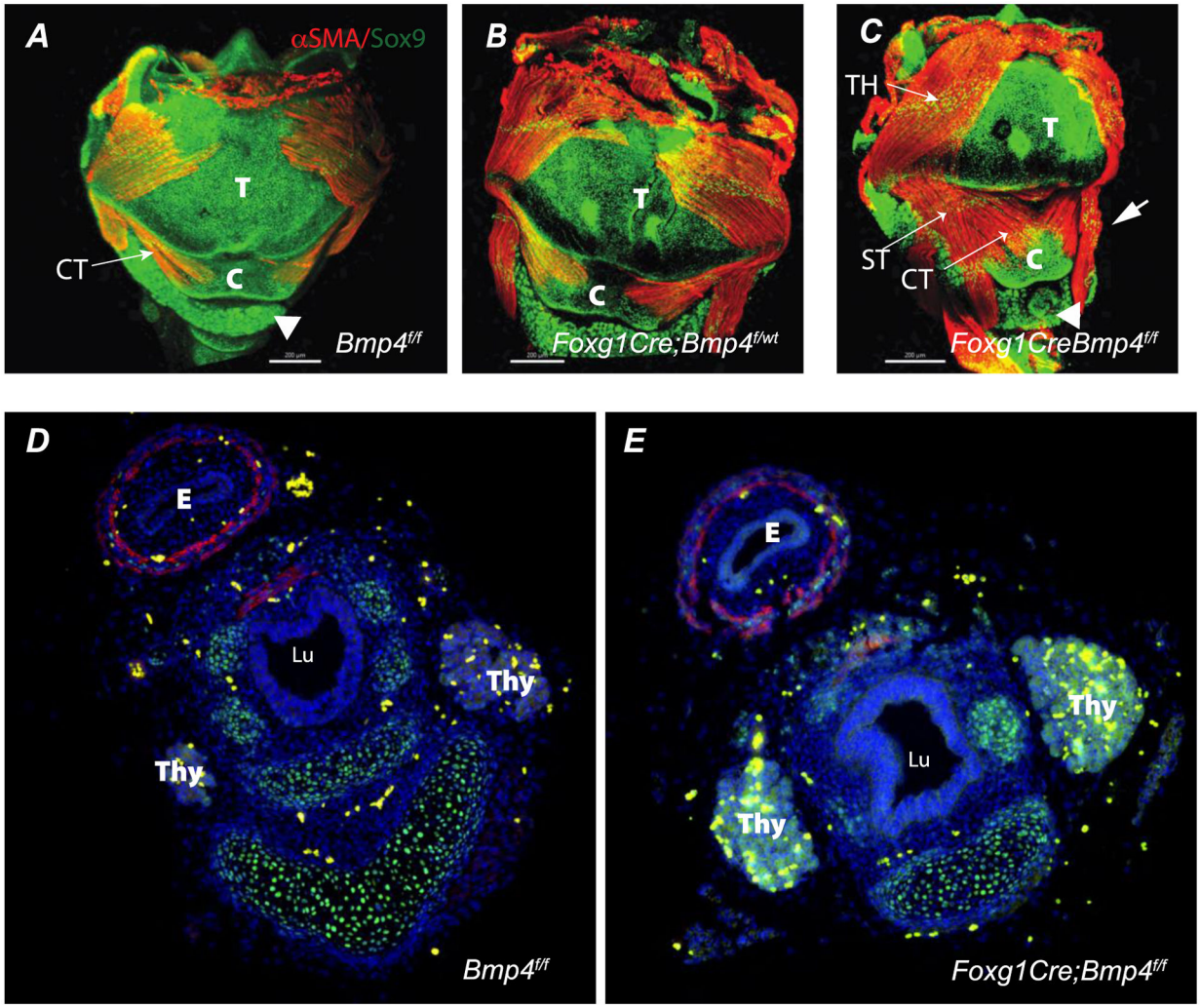

Figure 5:

Whole mount immunofluorescence of larynx at E16.5 (**A-C**) are shown. **A-C**: Ventral view of control (**A**) heterozygous (**B**), and mutant (**C**) larynx. Cartilage and muscle were detected in all genotypes analyzed as determined by positive immunofluorescence detection for Sox9 (green) and αSMA (red), respectively. Note in the mutant at E16.5 the anomalous appearance of the muscle and cartilaginous elements of the larynx (arrow in **C**) and the lower, more distal position of the thyroid (arrowhead in **C** vs **A** control). Panels **D** and **E** depict cross sections of E16.5 esophagus and distal larynx/upper trachea. Note the anomalous shape of the airway in the mutant. . TH= thyrohyoideus muscle, ST= sternohyoideus muscle, CT= cricothyroid muscle, E= esophagus, T= thyroid cartilage, C = cricoid cartilage, . Thy= Thyroid, Lu= Lumen. Scale bar = 200 μm.

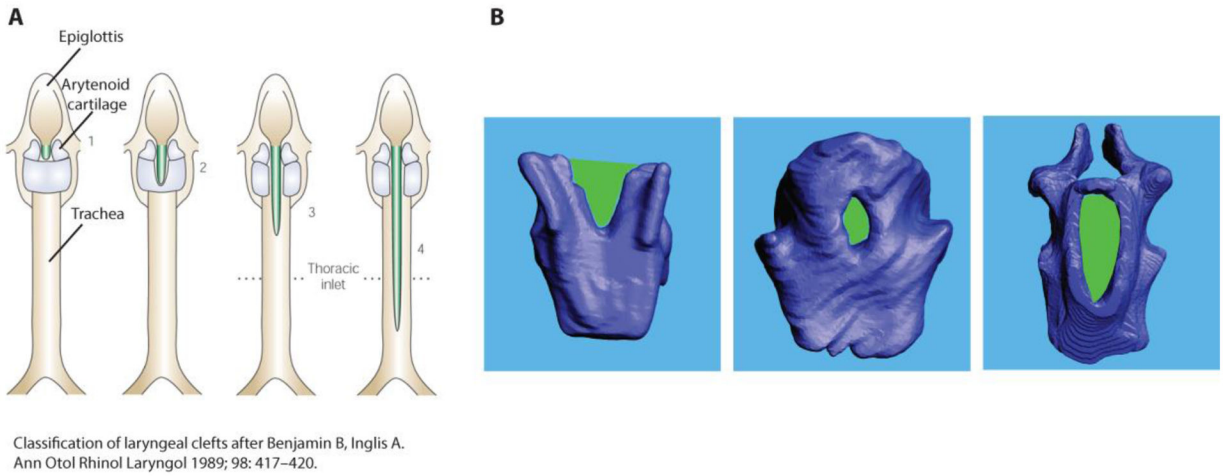

Figure 6:

Birth defects in the cricoid cartilage. **A**: Classification of laryngeal clefts after Benjamin and Inglis (1989). Shown are dorsal views of schematic images of the larynx and trachea. The green areas indicate varying degrees of gaps beginning between the arytenoid cartilages and reaching down the dorsal cricoid cartilage and the dorsal trachea. **B**: Dorsal views of cricoid cartilage reconstruction from three homozygote mice. The laryngeal cleft like malformation is outlined in green. Note also the ankylosis of both arytenoid cartilages with the cricoid cartilage in the specimen in the right panel.

Table 1:

Antibodies used for whole mount stainings.

Primary Antibody	Species	Dilution	Company	Catalog #
Anti Actin, Alpha Smooth Muscle-Cy3, monoclonal	Mouse	1:500	Sigma Aldrich	C6198
Anti Sox9, polyclonal	Rabbit	1:200	Millipore	AB5535
Secondary Antibody				
Anti Rabbit IgG (H+L), 488	Donkey	1:500	Invitrogen	A21206

Table 2:

Summary of qualitative description of laryngeal defects in three cartilages and the trachea. A total of 4 control (*Bmp4* $^{f/f}$) (+/+), 4 heterozygote *Foxg1Cre;Bmp4* $^{f/wt}$ (+/−) and 5 mutants *Foxg1Cre;Bmp4* $^{f/f}$(−/−) embryos were investigated. No defect was found in four control fetuses. One of the four heterozygous mutants showed a laryngeal malformation and all 5 homozygous mutants showed different laryngeal malformations. Findings for heterozygotes and mutants are explained. Numbers in parenthesis indicate the number of specimens in which the respective defect was observed. The defects are also illustrated in figure 2. As comparison for a normal shape, we used descriptions by Riede et al. (2020) for reference. CTJ: crico-Thyroid joint, CAJ: crico-arytenoid joint

Heterozygotes	Mutants
Thyroid cartilage: cartilage was fragile and asymmetric (n=1). Cricoid cartilage incomplete and asymmetric (n=1).	**Thyroid cartilage**: caudal horns are asymmetric in length and angulation toward the thyro-cricoid joint (n=2). **Cricoid cartilage**: Parts or complete cartilage is absent (n=3). There is a hole or gap/cleft in the dorsal cricoid lamina (n=4). Lateral horns which participate in CTJ are reduced and asymmetric; and the CTJ is malformed (n=2). Reduced facet which participates in CTJ (n=2). **Arytenoid cartilage**: Muscular process underdeveloped or absent (n=2). Cartilage is fused with cricoid cartilage in CAJ (n=2). **Trachea**: Only the cranial five tracheal rings are developed. Airway is collapsed caudal from the fifth tracheal ring (n=5).

Table 3:

Genes associated with laryngeal malformations in humans. A bibliographic search was performed in PubMed and publicly available databases. Mutations in members of essential signaling pathways, including Hedgehog (HH) and Retinoic Acid were found associated with laryngeal malformations in humans. Several genes in the list are also associated with complex syndromes affecting other cartilage, bones and different organs.

Condition	Gene	Citation (First author, DOI or database link)	Disease name	Other cartilage/ bone malform ations
Vocal cord palsy	GDAP1	Sevilla et al. 2008, 10.1093/brain/awn228	Charcot-Marie-Tooth	
Vocal cord palsy	MTMR2	Dragatsis et al. 2019, 10.3389/fnins.2019.00974	Charcot-Marie-Tooth	
Laryngeal cleft	MID1	De Falco et al. 2003, 10.1002/ajmg.a.10265; Bhoj et al. 2019, 10.1016/j.ejmg.2018.11.022; https://www.deciphergenomics.org/patient/271794/genotype/191579/browser	Opitz G/BBB syndrome	Yes
Laryngeal cleft	EDN1	Gordon et al. 2013, 10.1016/j.ajhg.2013.10.023	Auriculocondylar Syndrome	Yes
Laryngeal cleft - bifid epiglottis	GLI3	Johnston et al. 2010, 10.1002/humu.21328; Biesecker 2000–2022, Book chapter: https://www.ncbi.nlm.nih.gov/books/NBK1465/	Greig cephalopolysyndactyly, Pallister-Hall syndrome and Oral-Facial-Digital syndrome	Yes (skeletal dysplasia)
Laryngeal webs	HAAO	Shi et al. 2017, 10.1056/NEJMoa1616361; Szot et al. 2021, 10.1002/humu.24211	Vertebral, Cardiac, Renal, and Limb defects syndrome-1 (VCRL1)	Yes
Laryngeal webs - bifid epiglottis	BBS10	Poulin et al. 2019, 10.1016/j.ijporl.2019.04.019; Kaur et al. 2021, 10.1136/bcr-2020-236325;	Bardet-Biedl syndrome	
Bifid epiglottis	TTF2	Clifton-Bligh et al. 1998, 10.1038/1294	-	
Laryngomalacia	CHD7	Aramaki et al. 2006, 10.1016/j.jpeds.2005.10.044; Lau et al. 2020, 10.1136/bcr-2019-233037	coloboma, heart defects, choanal atresia, growth retardation, genital abnormalities, and ear abnormalities (CHARGE) syndrome	Yes (trachea)
Laryngomalacia	ALDH1A2	Leon et al. 2022, 10.1002/ajmg.a.62991	autosomal recessive ALDH1A2-deficient malformation syndrome	
Laryngomalacia	ARID1B	https://www.deciphergenomics.org/patient/276863/genotype/191212/browser; https://www.deciphergenomics.org/patient/258975/genotype/190368/browser; https://www.deciphergenomics.org/patient/277745/genotype/218707/browser; https://www.deciphergenomics.org/patient/260010/genotype/199882/browser; https://www.deciphergenomics.org/patient/260753/genotype/190376/browser; https://www.deciphergenomics.org/patient/265449/genotype/191152/browser; https://www.deciphergenomics.org/patient/294237/genotype/197577/browser; https://www.deciphergenomics.org/patient/261629/genotype/192877/browser	-	Yes
Laryngomalacia	MYT1L	https://www.deciphergenomics.org/patient/274566/genotype/210512/browser; https://www.deciphergenomics.org/patient/281321/genotype/211860/browser	-	

Condition	Gene	Citation (First author, DOI or database link)	Disease name	Other cartilage/ bone malform ations
Laryngomalacia	NIPBL	https://www.deciphergenomics.org/patient/260010/genotype/190455/browser (ARID1B mutation); https://www.deciphergenomics.org/patient/279612/genotype/198372/browser	-	
Laryngomalacia	KMT2A	https://www.deciphergenomics.org/patient/264500/genotype/191353/browser; https://www.deciphergenomics.org/patient/277208/genotype/208745/browser	-	Yes
Laryngomalacia	DYNC1H1	https://www.deciphergenomics.org/patient/262719/genotype/200259/browser (add. subglottic stenosis); https://www.deciphergenomics.org/patient/279605/genotype/193469/browser	-	
Laryngomalacia	PPM1D	https://www.deciphergenomics.org/patient/265370/genotype/197255/browser; https://www.deciphergenomics.org/patient/282974/genotype/198587/browser	-	Yes
Laryngomalacia	SMARCA4	https://www.deciphergenomics.org/patient/275756/genotype/191604/browser; https://www.deciphergenomics.org/patient/263032/genotype/210255/browser; https://www.deciphergenomics.org/patient/281321/genotype/211863/browser (MYTL1 mutation)	-	Yes
Laryngomalacia	ZC4H2	https://www.deciphergenomics.org/patient/280835/genotype/197289/browser; https://www.deciphergenomics.org/patient/296515/genotype/197553/browser	-	
Laryngotracheo-malacia	SOX9	Lee et al. 2011, 10.1002/dvg.20717	Campomelic Dysplasia	
Laryngotracheo-malacia	TAF1	https://www.deciphergenomics.org/patient/272400/genotype/217709/browser; https://www.deciphergenomics.org/patient/263481/genotype/197958/browser	-	Yes
Laryngeal ossification	DDR2	Bargal et al. 2009, 10.1016/j.ajhg.2008.12.004	Spondyloepimeta physeal dysplasia - short limb (SMED-SL)	Yes (trachea, ribs)
Laryngeal ossification and laryngeal cartilage malformations	GDF6	Clarke et al. 2021, 10.3390/genes12091354	Multiple synostoses syndrome type 4	Yes
Laryngospasm	GNA11	Zhang et al. 2021, 10.1016/j.endmts.2021.100106	Hypocalcaemia	
Larynx and trachea stenosis	FRAS1	Haelst et al. 2007, 10.1002/ajmg.a.31951	Fraser Syndrome	
Vascular ring, laryngeal web, laryngotracheo-malacia, and subglottic stenosis	chromosom e 22q11.2: TBX1	Kelly et al. 2004, 10.1093/hmg/ddh304; Haddad et al. 2019, 10.1186/s40842-019-0087-6	22q11.2d/Di George Syndrome	
Larynx hypoplasia	chromosom e 5p15.3	Mainardi 2006, 10.1186/1750-1172-1-33	Cri du chat syndrome	